Receptor-mediated Endocytosis of Asialoglycoproteins by Rat Liver Hepatocytes: Biochemical Characterization of the Endosomal Compartments

DORIS A. WALL and ANN L. HUBBARD
Department of Cell Biology and Anatomy, The Johns Hopkins University School of Medicine, Baltimore, Maryland 21205. Dr. Wall's present address is Department of Cell Biology and Anatomy, Cornell University Medical College, New York, New York 10020.

ABSTRACT The endocytic compartments of the asialoglycoprotein (ASGP) pathway in rat hepatocytes were studied using a combined morphological and biochemical approach in the isolated perfused liver. Use of electron microscopic tracers and a temperature-shift protocol to synchronize ligand entry confirmed the route of ASGP internalization observed in our previous in vivo studies (1) and established conditions under which we could label the contents of successive compartments in the pathway for subcellular fractionation studies. Three endosomal compartments were demonstrated in which ASGPs appear after they enter the cell via coated pits and vesicles but before they reach their site of degradation in lysosomes. These three compartments could be distinguished by their location within the hepatocyte, by their morphological appearance in situ, and by their density in sucrose gradients. The distributions of ASGP receptors, both accessible and latent (revealed by detergent permeabilization), were also examined and compared with that of ligand during subcellular fractionation. Most accessible ASGP receptors co-distributed with conventional plasma membrane markers. However, hepatocytes contain a substantial intracellular pool of latent ASGP binding sites that exceeds the number of cell surface receptors and whose presence is not dependent on ASGP exposure. The distribution of these latent ASGP receptors on sucrose gradients (detected either immunologically or by binding assays) was coincident with that of ligand sequestered within the early endosome compartments. In addition, both early endosomes and the membrane vesicles containing latent ASGP receptors had high cholesterol content, because both shifted markedly in density upon exposure to digitonin.

The endocytic pathway of galactose-terminating glycoproteins (ASGPs)[1] in rat hepatocytes begins with the binding of circulating ligand to cell surface receptors and internalization via coated pits and vesicles (1). The ligand rapidly appears in a prelysosomal system of smooth-membraned tubules and vesicles underlying the sinusoidal front membrane (peripheral endosomes) and then a short time later (~4 min) is found in tubular, vesicular, and multivesicular structures in the Golgi–lysosome region of the cell (internal endosomes). ASGPs are subsequently degraded within lysosomes, but the receptor to which they were originally bound at the cell surface is spared immediate degradation. Substantial indirect evidence indicates that each receptor is reused and can mediate the entry of >200 ligand molecules in its lifetime (2–4). To understand the mechanism by which hepatocytes can sort molecules destined for different intracellular fates, such as ASGPs and their receptor, more detailed information regarding the subcellular compartments involved in the endocytic pathway must be obtained.

This paper reports the results of a study of ASGP and receptor distribution after subcellular fractionation of rat livers that have been exposed to the ligand for brief times (2.5–10 min). Using an isolated perfused liver system, we have been able to perform temperature-shift experiments in which

[1] *Abbreviations used in this paper:* ASGP, asialoglycoprotein; ASOR, asialoorosomucoid; ASOR-HRP, ASOR-horseradish peroxidase; EM, electron microscope (microscopic).

THE JOURNAL OF CELL BIOLOGY · VOLUME 101 DECEMBER 1985 2104–2112

ligand entry was synchronized. Since normal liver structure is maintained (5), the well-established fractionation schemes for rat liver (6, 7) could be applied to the perfused tissue. Our morphological results demonstrate the appearance of ASGPs in three distinct prelysosomal (endosome) compartments. Two of these compartments (peripheral and internal tubular) have similar biochemical properties. We also present evidence documenting the existence of an internal pool of latent ASGP receptors, whose presence is not dependent upon ASGP exposure and which is found in a subcellular membrane compartment with biochemical properties similar to those of several of the endosome compartments traversed by the ligand. Portions of this work have been published in preliminary form (8).

MATERIALS AND METHODS

Materials

Reagents were purchased from the following sources: digitonin and polyethylene glycol (20,000 mol wt) from Sigma Chemical Co. (St. Louis, MO); bovine serum albumin (BSA) and human orosomucoid (α_1-acid glycoprotein) from Miles Biochemicals (Elkhart, IN); gold chloride from Fisher Scientific Co. (Fair Lawn, NJ); metrizamide from Accurate Chemical & Scientific Corp. (Westbury, NY); and chloramine T from Eastman Kodak Co. (Rochester, NY). Dye reagent concentrate for the Bio-Rad protein assay was obtained from Bio-Rad Laboratories (Richmond, CA). Male Sprague-Dawley rats (150–250 g) were obtained from Charles River Breeding Laboratories (Wilmington, MA). All other reagents were obtained from the same sources given in recent publications from this laboratory (1, 9) or were of the highest quality available.

Human orosomucoid was desialylated with insolubilized neuraminidase, and the resulting asialoorosomucoid (ASOR, >90% depleted of sialic acid) was iodinated using chloramine T (10). Specific radioactivities were $0.5–2 \times 10^7$ cpm/μg ASOR.

Isolated Liver Perfusion

The protocols for isolated liver perfusion and temperature-shift experiments have been described earlier (5, 11). In brief, the isolated organ was perfused for 60–90 min at 4°C with 5–10 μg ^{125}I-ASOR/g wet wt liver to saturate surface ASGP binding sites (11). After unbound ligand was rinsed away, the liver was warmed rapidly to 31–32°C by a single-pass perfusion with 37°C medium, bypassing the cold condenser. Return to low temperature was achieved by switching back to the recirculating perfusion mode and reattaching the (still cold) condenser. This procedure allowed the shift from high (31–32°C) to low temperature (4°C) or vice versa to be accomplished within 1.5 min. Surface-bound ligand was dissociated by a 10-min perfusion at 4°C with 10 mM EDTA, pH 7.4. Livers to be used for subcellular fractionation were perfused with 25–50 ml of the appropriate homogenization buffer at 2–4°C as the final step before homogenization. All livers were from animals starved 12–24 h before being killed.

Subcellular Fractionation

ISOLATION OF MEMBRANE FRACTIONS: Two initial subcellular fractions (12,000 *g* and microsomal pellets) were prepared by the method of Amar-Costesec et al. (7) as described in reference 12. The microsomes were further analyzed by isopycnic centrifugation. The exact volumes and densities used to make each gradient are given in the appropriate figure legends. Linear sucrose gradients of 25–27 ml were formed over a 4–5-ml cushion of 1.27 g/cc sucrose. Microsomes (5–7 ml) in 0.25 M sucrose, 3 mM imidazole-HCl, pH 7.4 (S/I), were applied to the top of the gradient and centrifuged to equilibrium (82,500 g_{av} for 12–15 h; Beckman SW 28 rotor, Beckman Instruments Inc., Palo Alto, CA), and 1–1.5-ml fractions were collected as described previously (12). Microsomes (made heavier by 0.02 g/cc with metrizamide) were floated into continuous gradients of metrizamide, and fractions were collected after centrifugation for 120 min at 82,500 g_{av}. All manipulations were performed in a cold room and all centrifugations were in a Beckman L5-50 or L5-65 ultracentrifuge.

DIGITONIN-SHIFT EXPERIMENTS: Digitonin treatment has been used to distinguish various components of a microsomal fraction (13). The concentration of digitonin needed to achieve a maximal shift in density without releasing all of the labeled endosomal content was determined for each experiment by titration. In brief, microsomal fractions were prepared from livers warmed to 31–32°C for 2.5 min after initially binding ^{125}I-ASOR to the surface of hepatocytes at 4°C. Aliquots (0.2 ml diluted to 2 ml with S/I) were mixed with varying amounts of a freshly prepared stock suspension of digitonin (0.2% wt/vol in H_2O) to give final concentrations ranging from 0.0025 to 0.04%. After incubation at 0°C for 15 min and sedimentation of the microsomes (106,500 g_{av} for 60 min), the amount of ^{125}I-ASOR released to the supernate was determined and plotted as a function of digitonin concentration. 0.01% digitonin proved to be optimal, because it produced a large shift in density in sucrose gradients yet retained ~55% of the sequestered ^{125}I-ASOR in a sedimentable form in the trial titration. Although lower amounts of digitonin released less ligand, they produced only a partial shift of the ^{125}I-ASOR-containing vesicles. In the actual experiment, 3 ml of microsomes were treated with digitonin as described above at the same protein-to-digitonin ratio (milligram per percent) as in the trial. Control microsomes were subjected to a similar treatment without digitonin. After centrifugation at 100,000 g_{av} for 90 min, both digitonin-treated and control microsomal pellets were resuspended in 8 ml of 0.25 S/I and applied to sucrose gradients as described above.

ASOR Binding Assays

GENERAL PROTOCOL: Binding activity was measured in 5–22 nM ^{125}I-ASOR, 12.5 mM HEPES, pH 7.4, 187.5 mM NaCl, and 6.25 mM $CaCl_2$, with or without 0.6% wt/vol BSA. Total binding was determined in the presence of 0.08 or 0.14% digitonin to permeabilize membrane vesicles. Binding to accessible receptors was determined in the absence of digitonin. Latent binding was assessed with comparable results in two ways: subtraction of accessible binding from total binding; or blockage of accessible sites with unlabeled ASOR, followed by addition of ^{125}I-ASOR together with digitonin to the assay mixture. Subcellular fractions (25 to 200 μl, or 6.75 to 1,450 μg protein) were incubated in a final volume of 0.4 ml at 4°C with agitation for 60–120 min, and the reaction was stopped by the addition of 3 ml of cold rinse buffer (50 mM Tris-HCl pH 7.4, 300 mM NaCl, 10 mM $CaCl_2$, 0.1% BSA). The membrane fractions were then collected by filtration under vacuum on glass fiber filters (GF/C, Whatman Chemical Separation Inc., Clifton, NJ) presoaked with rinse buffer. After three rapid rinses with >30 ml of buffer, the radioactivity present on the dried filters was measured (Beckman Gamma 4000). Nonspecific binding was determined by addition of unlabeled ASOR (100–250-fold excess over ^{125}I-ASOR) just before the addition of ^{125}I-ASOR and was routinely 0.2–0.5% of the added radioactivity.

CHOICE OF ASSAY CONDITIONS: The inclusion of 0.14% digitonin resulted from preliminary binding assays in which detergent level was varied from 0 to 0.6% using either a homogenate or microsomal fraction. The maximal increase in binding to microsomal fractions observed with digitonin was 2.8- to 5.3-fold over the levels seen without digitonin. 0.08% digitonin was found to be optimal for measuring binding activity in gradient fractions, due to the lower amounts of protein in these fractions. The shape and position of the peak of ASGP binding activity in a given gradient were similar regardless of the digitonin level used (0.08 or 0.14%), the only difference being the absolute number of binding sites detected.

Titration of the amount of ASOR added to either homogenate or plasma membrane fractions indicated that the amount of ASOR routinely used was below saturating levels for our in vitro assay and gave receptor numbers 1.5–4 times lower than the maximum values obtained at saturating ASOR concentrations (~50 nM). It is not currently clear why such high levels of ligand must be used to saturate binding in our in vitro assay, since the dissociation constant for the ASGP receptor is in the nanomolar range (2). Nevertheless, the distribution of binding activity throughout a gradient or a given fractionation scheme was similar regardless of the amount of ASOR used (data not shown). Nonspecific binding was 1–16% of specifically bound radioactivity for total binding to the peak gradient fractions. The amount of ligand binding measured in the assay described above (i.e., in the presence of digitonin and 0.6% BSA) gave equal or slightly higher values than that measured by the procedure of Hudgin et al. (14), which includes Triton X-100 solubilization and ammonium sulfate precipitation (either with or without BSA).

Antibody to the ASGP Receptor

PREPARATION: ASGP receptor was purified by affinity chromatography according to the method of Hudgin et al. (14). The receptor preparation was electrophoresed on preparative SDS polyacrylamide gels (SDS PAGE [15]), and the major Coomassie Blue–staining band at 42,000 M_r was cut out. After electroelution (16) and analysis by SDS PAGE, an estimated 100 μg of the preparation was emulsified in complete Freund's adjuvant and injected at multiple intradermal sites into rabbits. A booster injection (50 μg) was given 2 wk later, and blood was collected every 2 wk thereafter.

DETECTION OF ASGP RECEPTORS IN FRACTIONS: Aliquots of su-

crose gradient fractions containing 50 μg protein each were solubilized as described (17) and applied to 8.5% SDS polyacrylamide gels. After electrophoresis, the proteins were transferred to nitrocellulose (18), and the blot was incubated with antireceptor antiserum (1/1,000) followed by ^{125}I-protein A as described (19, 20). The immunoblots were processed, and the resulting autoradiograms were analyzed as described (21).

Other Biochemical Determinations

Protein was assayed by the Bio-Rad procedure (22), using bovine γ-globulin as a standard. 5′-Nucleotidase and β-*N*-acetylglucosaminidase activity were assayed as described (17, 23, 24).

Degradation products of ^{125}I-ASOR were detected by precipitation of 0.5 ml of sample in 0.25 M sucrose or perfusate medium in 10% trichloroacetic acid. After 60 min on ice, samples were centrifuged (1,800 g_{av} for 25 min), and the radioactivity present in the supernates and pellets was measured.

Electron Microscopy (EM)

ASOR-PEROXIDASE VISUALIZATION: The preparation and visualization of a covalent conjugate between ASOR and horseradish peroxidase (ASOR-HRP) and quantitation of ASOR-HRP-containing structures in peripheral and Golgi-lysosomal regions have been described (1).

ASOR-COLLOIDAL GOLD PREPARATION: Colloidal gold was prepared by reduction of gold chloride with 2.5 mM $NaBH_4$ in 1 mM K_2CO_3, pH 9 (25). ASOR (20 μg/ml) plus a trace amount of ^{125}I-ASOR were adsorbed to the gold colloid by adding the proteins at pH 9 and subsequently lowering the pH to 6. 5 min later, the ASOR-gold colloid complex (ASOR-Au) was neutralized with phosphate-buffered saline, pH 7.5, and stabilized by the addition of polyethylene glycol to a final concentration of 0.2%. The gold particles were centrifuged at 157,000 g_{av} for 90 min and subsequently fractionated into different size classes on 10–30% glycerol gradients (26). 29–62% of the ASOR initially added was adsorbed to the gold particles. Only material of 5–10-nm diam from the upper half of the gradients was used for the localization experiments.

USE OF DENATURED BSA IN ASOR-AU: Denatured BSA was prepared (27) and 20–30 mg was added to the perfusion medium 10–15 min before the addition of ASOR-Au to minimize nonspecific binding of the particulate colloidal gold tracer to sinusoidal lining cells (unpublished observation).

FIXATION AND PROCESSING OF FRACTIONS AND TISSUE: Subcellular fractions (50–200 μl) were fixed as described previously (9). In some EM tracer experiments, a biopsy was taken before homogenization of the remaining tissue for subcellular fractionation. The tissue fragment was cut into cubes (~3 mm^3) while immersed in cold fixative (2.5% glutaraldehyde, 1.5% formaldehyde, 0.1 M Na cacodylate, pH 7.4, 2.5 mM $CaCl_2$; reference 24). After 2–3 h, the cubes were minced into pieces of ~1 mm^3, placed into fresh fixative for another 60 min on ice, then processed as described (9).

RESULTS

ASOR-HRP and ASOR-Au Internalization by the Perfused Liver

We first used the EM tracers ASOR-HRP and ASOR-Au to establish the kinetics of ligand movement through the various compartments of the ASGP pathway in the perfused liver and, thus, to select conditions that would preferentially label the contents of endocytic vesicles at early or late times after ASGP internalization. The results of a temperature-shift study in which isolated perfused livers were warmed to 32°C for up to 15 min after 4°C binding of ASOR-HRP to cell surfaces are presented in Fig. 1 and Table I. The ligand movement in the isolated system faithfully replicated our earlier in vivo findings qualitatively (Fig. 1) and quantitatively (Table I). In brief, at the earliest times examined (1.5–3.5 min), at least 88% of all labeled structures were found within 1.5 μm of the sinusoidal plasma membrane and included pit and vesicle profiles (<100-nm diam) as well as tubules and vesicles that exhibited a variety of shapes and sizes (peripheral endosomes, Fig. 1, *a* and *c*). Perfusion with EDTA at 2 min did not eliminate tracer in coated structures (Table I). As early as 5 min after warming, half of the labeled structures were deeper in the cell and included tubules and vesicles similar morphologically to those at the periphery, as well as larger (200–500-nm diam) bodies containing small membrane vesicles and/or other inclusions that did not have limiting membranes (Fig. 1, *b* and *d–f*). This shift was largely completed by 15 min, when 90% of the total ASOR-HRP-containing structures were internal endosomes found in the Golgi-lysosome region. When ASOR-Au was used, both the kinetics of movement and the types of structures labeled were similar to those seen with the peroxidase tracer (Fig. 1, *c–f*). Although the ligands were present in a lysosome-rich area of the hepatocyte cytoplasm by 5–15 min, no detectable release to the medium of ^{125}I-ASOR as acid-soluble material was seen in the perfused liver until 25 min at 31–32°C (slightly later than in vivo [1], due to the lower temperature). This result suggested that between 5 and 15 min the endocytosed molecules in the Golgi-lysosome region were in structures other than functioning lysosomes.

Subcellular Fractionation After Labeling of Peripheral Endosomes

ANALYSIS OF INITIAL FRACTIONS: Based on the morphological data described above, a 2.5-min shift to 31–32°C was chosen as the standard time for labeling the contents of endosomes in the peripheral cytoplasm. Under the conditions chosen, 70 ± 8% (13 experiments) of the ^{125}I-ligand bound at 4°C was inaccessible to EGTA dissociation by 2.5 min, a time when >90% of the internalized EM tracers were still in the peripheral cytoplasm (Table I).

Two membrane fractions were prepared, and the distributions of ^{125}I-ASOR, marker enzymes, and ASGP binding activity were determined (Table II). The vast majority of both ^{125}I-ASOR and ASGP binding activity (measured in the presence of 0.14% digitonin) was recovered in the microsomal fraction, which also contained substantial amounts of the lysosomal marker, β-*N*-acetylglucosaminidase (20%) and the plasma membrane marker, 5′-nucleotidase (28%). That more than 90% of the ^{125}I-ASOR in all fractions was sedimentable indicates its association with membranous structures.

The microsomal fraction was clearly very heterogeneous in composition. Therefore, we applied two approaches to further resolve the components: application to sucrose gradients, and an examination of the effect of digitonin treatment on the density of various microsomal components.

SUCROSE GRADIENTS: After sedimentation of the microsomes in sucrose gradients, the endocytic vesicles labeled by a 2.5-min temperature shift were found in a single peak centered at a density of 1.12–1.13 g/cc, which was well separated from the bulk of microsomal protein near the bottom of the gradient (Fig. 2). The densities of the markers for plasma membrane (5′-nucleotidase; peak density, 1.15 g/cc) and lysosomes (β-*N*-acetylglucosaminidase; peak density, 1.178 g/cc) were heavier than that of the peripheral endosome peak.

We next examined the distribution of ASGP binding activity across this sucrose gradient (Fig. 3*A*). The binding assays were performed in both the presence and the absence of a high concentration of digitonin (0.14%) in order to distinguish receptors exposed to the medium (accessible receptors) from those oriented toward the luminal side of membrane vesicles (latent receptors). It is important to note that the values for

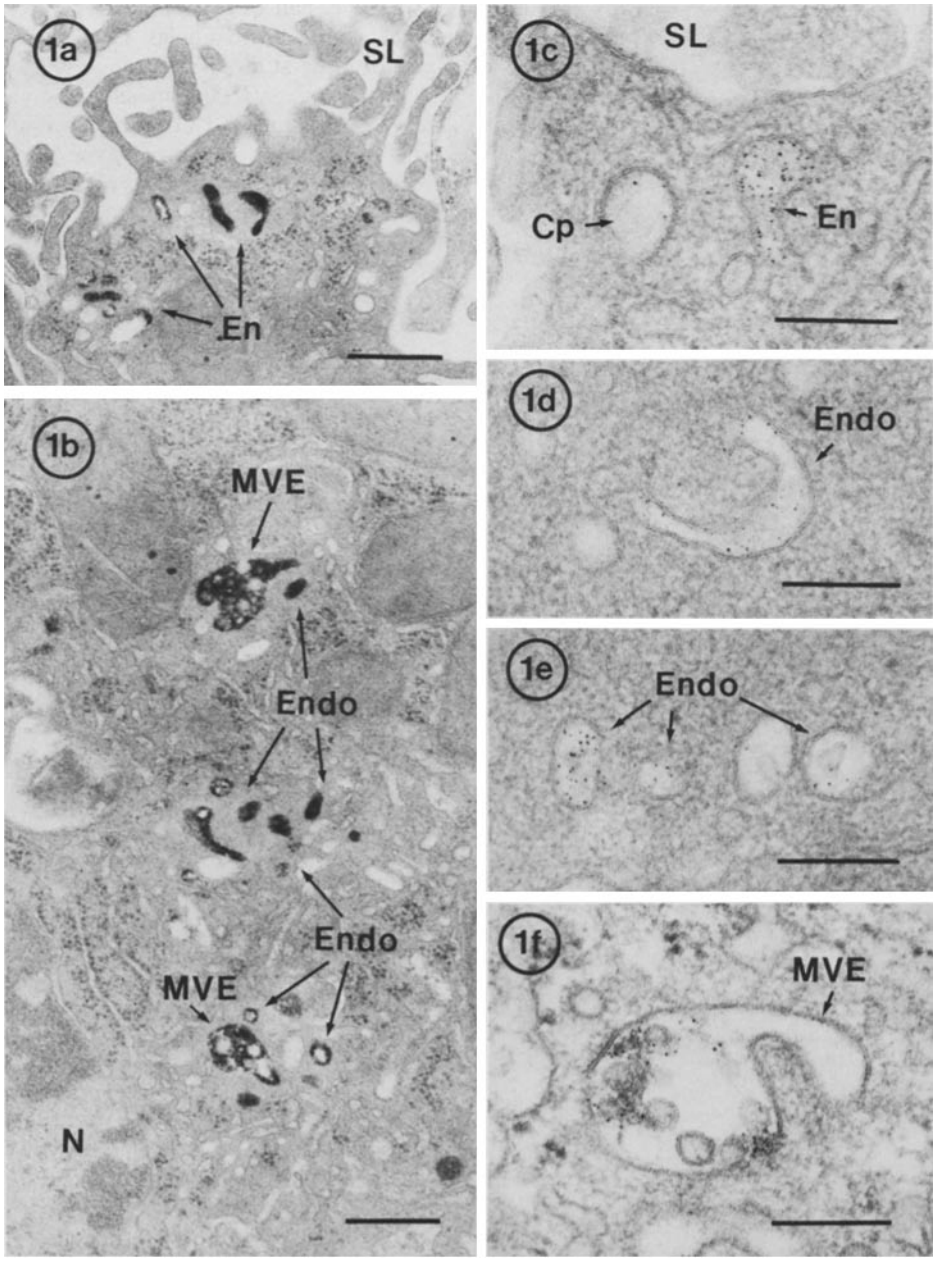

FIGURE 1 Electron micrographs of portions of hepatocytes containing endosomes labeled after internalization of ASOR-HRP (*a*, *b*) and ASOR-Au (*c–f*) by the perfused liver. Ligands (120 μg ASOR-HRP or 100 μg ASOR-Au) were bound to the surface of hepatocytes for 60 min at 4°C, excess ligand was rinsed out, and the livers were then warmed to 31–32°C for varying times. The liver containing ASOR-HRP tracer was fixed by perfusion in 2% glutaraldehyde. A portion of the ASOR-Au-containing liver was fixed by immersion as described in Materials and Methods. (*a*) Peripheral endosomes (*En*) containing ASOR-HRP are seen near the sinusoidal lumen (*SL*), among unlabeled smooth-membrane vesicles and tubules. The liver was warmed for 5.5 min. Bar, 0.5 μm. × 25,000. (*b*) Internal endosomes (*Endo*) and MVEs in the Golgi-lysosome region, near the nucleus (*N*). The liver was warmed for 7.5 min. Bar, 0.5 μm. × 25,000. (*c*) A peripheral endosome vesicle (*En*) and a coated pit (*Cp*) labeled with ASOR-Au are seen in the sinusoidal periphery of an hepatocyte. ASOR-Au is in close association with the membranes of coated pits but appears scattered in the lumen of the endosome. The liver was warmed for 2.5 min. Bar, 0.2 μm. × 80,000. (*d–f*) Internal endosomes (*Endo*) (tubulo-vesicular) (*d*, *e*) and MVEs (*f*) containing ASOR-Au in the Golgi-lysosome region of hepatocytes. Small vesicles and other particles found in the lumen of multivesicular endosomes are seen in *f*. The liver was warmed for 12 min. Bar, 0.2 μm. × 80,000.

the number of receptors should not be regarded as absolute, since ligand levels were subsaturating in the receptor assay of gradient fractions (see Materials and Methods).

Total ASOR binding activity seen in the presence of digitonin formed a single peak at a density similar to that of the peripheral endosome peak, with a shoulder extending into denser regions of the gradient. Binding activity measured in the absence of digitonin was substantially lower and had a very different distribution. The bulk of the accessible ASGP binding activity was between 1.13 and 1.15 g/cc sucrose, which suggests that plasma membrane receptors contributed significantly to the population of vesicles that have exposed binding sites. Multiple lines of evidence indicate that the hepatocyte plasma membrane vesiculates outside-out during homogenization (e.g., references 19 and 21). Finally, the distribution of latent ASGP binding sites was not the result of receptor internalization together with its ligand, because the same pattern of binding activity was obtained from microsomes prepared from livers perfused in the absence of ligand (data not shown).

DIGITONIN TREATMENT OF MICROSOMES: The coincidence of the peripheral endosome peak and that of latent ASGP binding activity prompted us to assess the behavior of the two components by the digitonin-shift technique of Amar-Costesec et al. (13). Vesicles whose membranes contain relatively large amounts of cholesterol bind more digitonin and are shifted in density to a greater extent than vesicles whose membranes have lower amounts of cholesterol. A concentration of 0.01% digitonin was chosen for these experiments. It represented a compromise between lower levels, which minimized loss of ligand, and higher levels, which gave an increased shift in density but also a greater loss of sequestered ligand (see Materials and Methods). After digitonin (or mock) treatment and sucrose gradient centrifugation the distributions of ligand and ASGP binding activity were determined (Fig. 3). Exposure of microsomes to digitonin resulted in a

TABLE I. *Time Course of ASOR-HRP Uptake After Temperature Shift*

Time of warming to 31–32°C (Total structures counted)	Intracellular region (% of total structures)		
	Peripheral cytoplasm		Golgi-lysosome region
	Pits and small vesicles*	Peripheral endosomes‡	Internal endosomes‡
1.5 min (69)	68	32	0
2 min (178)	39§	57	4
3.5 min (241)	39	49	12
5.5 min (440)	15	34	51
15 min (204)	1	7	92

* Category may contain some peripheral endosomes since coats were not visible in this material.

‡ Endosomes were classified as follows: peripheral endosomes were those labeled structures that were located <1.5 μm from the sinusoidal membrane, <200 nm in diam, and had the appearance of vesicles or tubules; internal endosomes were labeled structures that were located in regions rich in lysosomes and Golgi stacks, usually near bile canaliculi, and had two distinct morphologies—vesicles and tubules similar to those at the periphery, and larger (>200-nm diam) vesicles that contained smaller vesicles or other inclusions within the lumen.

§ EGTA dissociation of surface-bound ligand before fixation in this experiment resulted in a depletion of this category by eliminating staining of coated pits.

TABLE II. *Subcellular Distribution of ^{125}I-ASOR in Microsomes Labeled by a 2.5-min Temperature Shift*

Parameter	Percentage of homogenate		
	10,000 g (10 min) pellet	Microsomal pellet	Nonsedimentable
Sequestered ^{125}I-ASOR (4)*	6	84	9
ASOR binding activity (2)	18	79	3
β-*N*-Acetylglucosaminidase (3)	78	20	5
5′-Nucleotidase (4)	62	28	6

* Number of experiments.

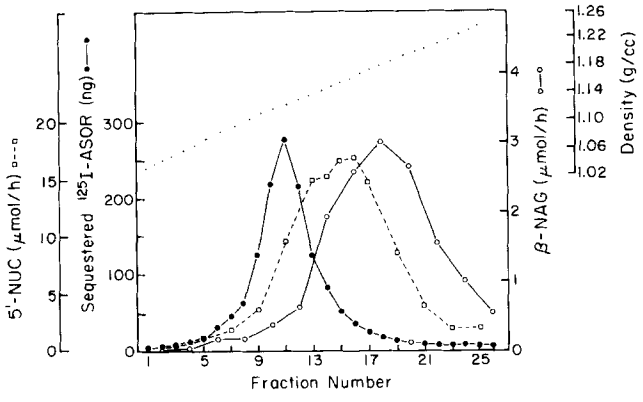

FIGURE 2 Sucrose gradient fractionation of microsomes labeled by a 2.5-min temperature shift. The contents of peripheral endosomes were labeled by exposure of an isolated perfused liver to ^{125}I-ASOR using a 2.5-min temperature-shift protocol (see Materials and Methods). 6.5-ml of a microsomal fraction in S/I was applied to the top of a 1.08–1.22 sucrose gradient (26.5 ml) over a 1.26 g/cc sucrose cushion (4.5 ml). Collected fractions were analyzed for sequestered ^{125}I-ASOR, 5′-nucleotidase (*5′-NUC*) activity, and β-*N*-acetylglucosaminidase (*β-NAG*) activity. Protein was found predominantly in fractions 17–25 (>1.16 g/cc) (data not shown).

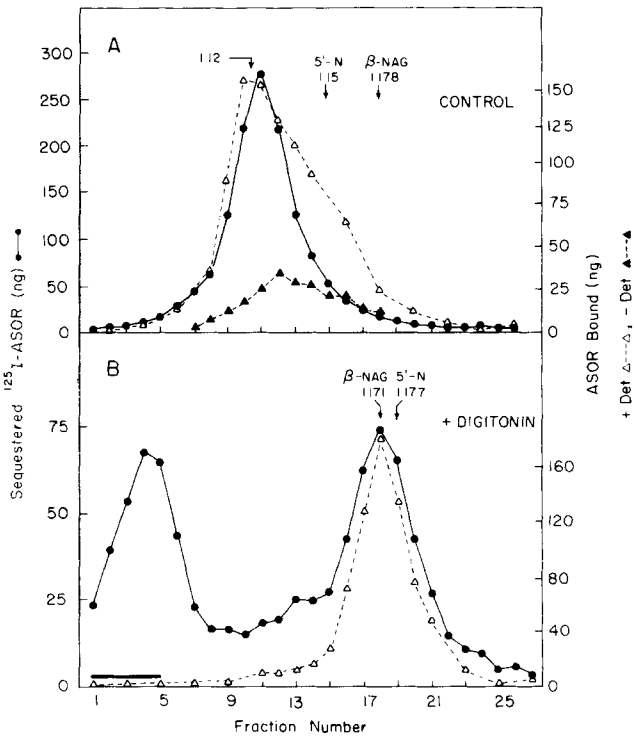

FIGURE 3 Distribution of the components of a microsomal fraction on sucrose gradients. The contents of peripheral endosomes were labeled using the 2.5-min temperature-shift protocol. 6.5 ml of a microsomal fraction in 0.25 M S/I (without [*A*] or with [*B*] prior digitonin treatment) were applied on top of 1.08–1.22 g/cc linear sucrose gradients (26.5 ml) over a cushion of 1.26 g/cc sucrose (4.5 ml). The gradients were centrifuged, collected, and analyzed as described in Materials and Methods. (*A*) Control microsomes. Both sequestered ^{125}I-ASOR (●) and total ASGP binding activity (Δ) measured at ~40% saturation, showed similar density distributions, except for a shoulder of binding activity on the heavy side of the 1.12 g/cc peak. Accessible ASGP binding activity measured in the absence of detergent (▲) distributes at higher densities than does total ASGP binding activity. (*B*) Effect of digitonin treatment. Microsomes were exposed to 0.01% digitonin as described in Materials and Methods. ^{125}I-ASOR exhibits two peaks: the material at the top of the gradient is nonsedimentable ligand released during the digitonin exposure (marked by bar); ligand at 1.17 g/cc is sequestered within peripheral endosomes that have shifted from the density of 1.12 g/cc in controls (*A*) as a result of the digitonin treatment. Total ASGP binding activity exhibits the same shift as does the endosome peak. The peak densities of vesicles containing 5′-nucleotidase (*5′-N*) and β-*N*-acetylglucosaminidase (*β-NAG*) are indicated by arrows.

parallel shift in the distributions of both the ^{125}I-ASOR and ASGP binding activity from a control density of 1.12 g/cc (Fig. 3*A*) to 1.17 g/cc (Fig. 3*B*). The ^{125}I-ASOR released during sedimentation (~50% of the total radioactivity applied to the gradient) was seen at the top of the gradient where the sample was applied. The extent of the shift seen for the peripheral endosomes and binding activity was greater than that of the plasma membrane 5′-nucleotidase (from 1.15 g/cc in the control to 1.177 g/cc after digitonin exposure) or for the lysosomal marker β-*N*-acetylglucosaminidase (virtually no shift after digitonin exposure).

To rule out the possibility that released ^{125}I-ASOR had bound to unoccupied receptors (despite the absence of calcium in the fractionation), we prepared microsomes from a

naive liver (i.e., one not perfused with ligand) and added exogenous ^{125}I-ASOR during both digitonin treatment and subsequent centrifugations. Virtually none of the ^{125}I-ASOR entered the gradient, and its distribution was markedly different from that of total ASGP binding activity, which was shifted by the digitonin treatment to an extent comparable to that shown in Fig. 3*B* (data not shown). We therefore concluded that rebinding of released ligand was not a significant problem.

Finally, electron microscopic examination of microsomal fractions treated with as much as 0.14% digitonin did not reveal any abnormalities of vesicle size or overall appearance, which suggests that vesicle fusion had not occurred (data not shown).

ASGP BINDING ACTIVITY VS. ASGP RECEPTOR MOLECULES: The use of binding assays allows detection of only active receptors capable of ligand association and may not reveal the presence of inactive receptors that cannot bind ligand. We therefore determined the subcellular distribution of ASGP binding activity at both subsaturating and saturating levels of ligand and compared this with the distributions of receptor protein detected immunologically with anti-ASGP receptor antibodies and with ^{125}I-ASOR sequestered in peripheral endosomes (after a 2.5-min warm-up). The immunoblot analysis is presented in Fig. 4. Receptor protein was found in the same fractions as binding activity, measured at 12 or 140 nM ASOR, and all were coincident with distribution of sequestered ^{125}I-ASOR. These results indicated that the vast majority of hepatocyte ASGP receptors resided in a membrane fraction of low density, regardless of the means of receptor detection.

Subcellular Fractionation of Livers Labeled for >2.5 Min

Based on our morphological data described above (Table I), we chose a 10-min warm-up protocol to label predominantly the internal endosomes, and then we fractionated liver homogenates. The distribution and recoveries of sequestered ^{125}I-ASOR and ASGP binding activity in the initial fractions were comparable to those seen after warming for 2.5 min (see Table II). However, sucrose gradient analysis of the microsomes revealed a greater proportion of the sequestered ^{125}I-ASOR in lighter regions of the gradients (Fig. 5). These lighter endosomes appeared as a small peak or shoulder with a density of ~1.07 g/cc, whereas the main endosome peak remained at ~1.12–1.13 g/cc (the same position as the single 2.5-min peak). In contrast, the density distribution of the ASGP binding peak (total activity measured in the presence of 0.14% digitonin) was unchanged from that seen after 2.5-min warming. The new, lighter peak of sequestered ^{125}I-ASOR was well separated from the bulk of lysosomal enzyme activity, although a low level was detectable in the light region. This separation was consistent with the lack of detectable ligand degradation after a 10-min temperature-shift.

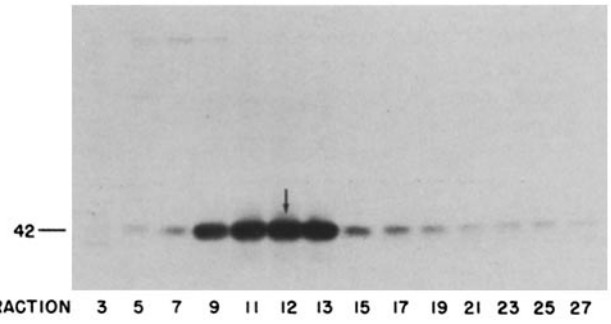

FIGURE 4 Immunoblot analysis of ASGP receptor in sucrose gradient fractions. The contents of peripheral endosomes were labeled using the 2.5-min temperature-shift protocol; microsomes were prepared and subfractionated on a sucrose gradient of composition similar to that described in Fig. 2. Collected fractions were analyzed for binding activity with 12 and 140 nM ASOR, receptor protein on immunoblots, and sequestered ^{125}I-ASOR. Only the autoradiogram of the immunoblot is presented, with the peaks of the other three distributions indicated by an arrow at 1.12 g/cc. The distributions were superimposable.

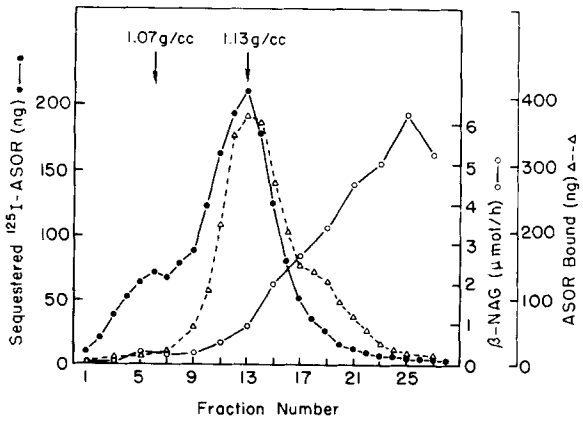

FIGURE 5 Sucrose gradient fractionation of microsomes labeled by a 10-min temperature shift. The contents of internal endosomes were labeled by exposure of an isolated perfused liver to ^{125}I-ASOR using a 10-min temperature-shift protocol (see Materials and Methods). Microsomes (27% of the ^{125}I-ASOR in the homogenate) in 0.25 M S/I were subfractionated on a 1.06–1.20 g/cc linear sucrose gradient (28.5 ml) with a cushion of 1.27 g/cc sucrose (4.5 ml). The distribution of ^{125}I-ASOR sequestered within endosomes is biphasic, with a major peak at 1.13 g/cc and a minor one at 1.07 g/cc. Total ASGP binding activity, measured at ~45% saturation, is associated with vesicles equilibrating at densities similar to those from 2.5-min livers (compare Fig. 3), with a major peak at 1.13 g/cc and a shoulder on the heavy side.Very little β-*N*-acetylglucosaminidase activity is seen in the region of the light endosome peak (predominantly MVEs: see Fig. 6, *e* and *f*).

The morphology of fractions containing the heavier and lighter endosomes was examined after exposing livers to ASOR-Au for 10 min and then subfractionating the microsomes on metrizamide gradients (where better morphology was obtained than in sucrose). A liver biopsy, taken for in situ morphology, confirmed that >75% of all ASOR-Au was located in the internal regions of the cell. The distribution of either the gold tracer (^{125}I-ASOR-labeled) or ^{125}I-ASOR on metrizamide was similar to that found in sucrose gradients (data not shown). ASOR-Au particles were found in both tubules and small vesicles with single limiting membranes in fractions at 1.10 g/cc (Fig. 6, *a–d*). The labeled structures in the lighter density region were larger (200–500-nm diam) and usually filled with smaller vesicles and other particles of moderate electron density (Fig. 6, *e* and *f*). They corresponded in appearance to the multivesicular endosomes found in the internal regions of hepatocytes in situ (Fig. 1*f*).

DISCUSSION

The intracellular pathway taken by ASGPs appears to be

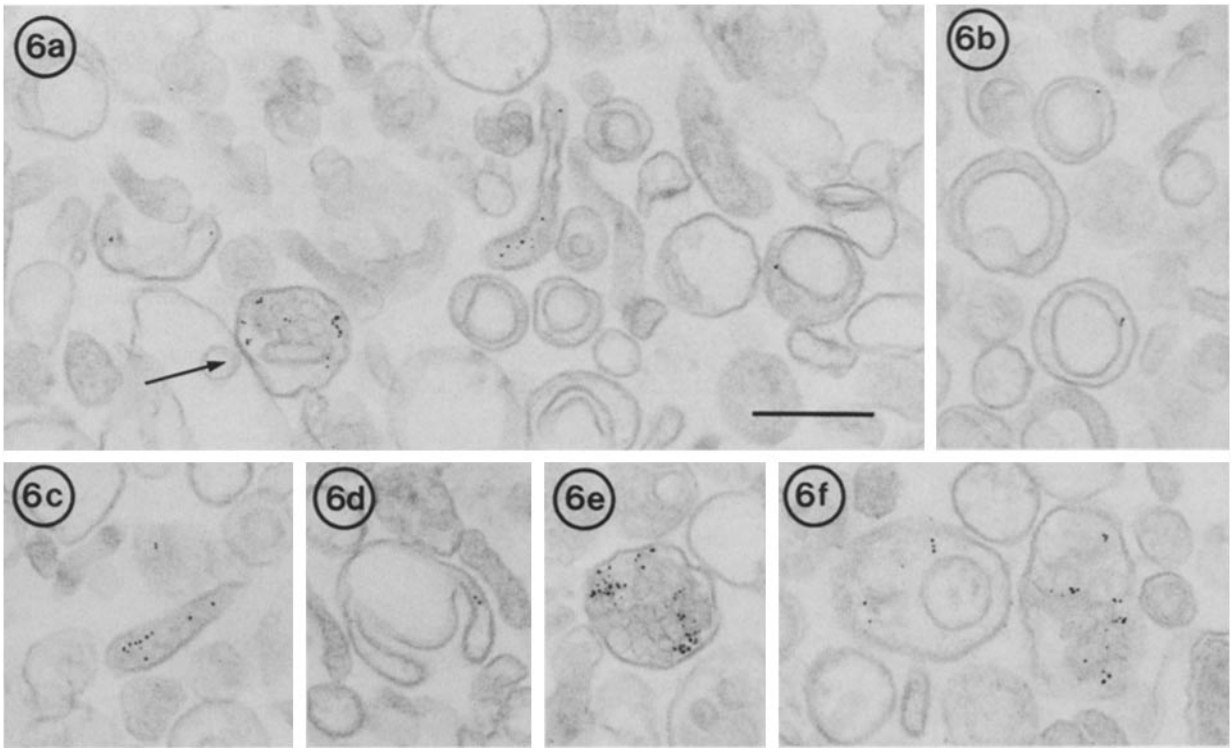

FIGURE 6 Electron micrographs of material from metrizamide gradient fractions containing ASOR-Au sequestered in internal endosomes. A 10-min temperature-shift protocol was used to internalize ASOR-Au into hepatocytes. Microsomes (at 1.19 g/cc) were floated into a continuous gradient of metrizamide (1.07–1.17 g/cc), and fractions were collected and analyzed as described in Materials and Methods. Fractions of density 1.10 g/cc (*a–d*) and 1.07 g/cc were examined (*e, f*). In the denser fractions, the gold tracer is seen primarily in endosomes consisting of tubular structures (*a* and *c*), annular profiles (*b*), and in apparently empty bodies with projecting arms (*d*). Occasionally more complex bodies containing small membrane vesicles and/or other inclusions (MVEs) are found in the denser gradient region (indicated by an arrow in *a*). MVEs are the predominant ASOR-Au-containing structure in the light gradient regions (*e, f*). Their average size is larger than that of similar vesicles seen at 1.10 g/cc (200 to 500 nm at 1.07 g/cc vs. 100–200 nm at 1.10 g/cc). Bar, 0.2 μm. × 80,000.

shared by other ligands destined for lysosomal degradation and is found in many cell types (reviewed in reference 28). Although the beginning (coated pits-vesicles) and end (lysosomes) of this pathway have been identified in virtually all cells, the discrete elements of the intervening endosomal compartment are most clearly revealed in a polarized epithelial cell such as the hepatocyte. In this study we combined morphological and biochemical approaches to analyze the three endosomal compartments of the ASGP pathway. The results we have obtained extend our own earlier observations (1) and those of others (e.g., reference 29) and provide a foundation for further examination of the role of endosomes in sorting.

Morphological and Geographical Relationships

After their internalization via coated pits and vesicles, ASGPs enter peripheral endosomes, which consist of small uncoated vesicles and tubules. As the ligand moves into the Golgi-lysosome region of the hepatocyte, it appears simultaneously in vesicles and tubules that often show extensive interconnections (internal endosomes) and in large bodies (multivesicular endosomes [MVEs]) that contain smaller vesicles and inclusions reminiscent of lipoprotein particles. The tubules of the internal endosomes frequently appear to be attached to the MVEs. The latter structures appear similar to the multivesicular bodies implicated in the endocytic pathways of other cell types (30–36); however, in liver, lipoprotein particles are also present in MVEs and are probably of endocytic origin (36).

Biochemical Relationships

We found all elements of hepatocyte endosomes to be of lower average density than most subcellular organelles, except for Golgi elements (32, 37), and therefore readily separated from the bulk of microsomal protein. This result has been reported in studies of endocytic vesicles in liver (29, 30, 38–40) and in other cell types (e.g., references 41–43). However, in the present study we were able to identify more precisely the specific endosomal subcompartment being analyzed, through use of the isolated perfused liver and correlations between the in situ morphological distribution of internalized ASGPs and the biochemical distribution of isolated, labeled components. For example, we have found that peripheral (2.5 min) and internal (10 min) tubular-vesicular endosomes have the same buoyant densities in sucrose (~1.12 g/cc; Figs. 2 and 4) and metrizamide (~1.10 g/cc; data not shown). Therefore, they may be components of a single membrane system, with discrete elements found in different cellular regions. However, the morphology of the two types of endosomes in situ is somewhat different, with a greater tendency toward interconnected branching structures in the internal tubular endosomes of the Golgi-lysosome region. Whether this morphological difference is correlated with biochemical differences in the membranes remains to be determined. In addition, we iden-

tified biochemically an endosome that was both lighter and accumulated ligand later than the tubular elements. Again, using morphological tracers, we found these to be MVEs. This last subcompartment of the endosomal system (MVEs) appears to be the fraction isolated by Quintart et al. using ligand-induced density modification (29, 44). The virtual absence of several enzyme markers assayed (e.g., galactosyl transferase, alkaline phosphodiesterase, and 5′-nucleotidase) suggests that considerable membrane sorting may occur before entry of ligand into MVEs. However, the presence (or absence) of plasma membrane antigens known to be specific to the blood sinusoidal domain of hepatocytes (the origin of the pathway), and of receptors and other membrane molecules possibly relevant to endocytosis and sorting (e.g. a proton-ATPase [45]), was not assessed. Results presented here (Figs. 5 and 6, *e* and *f*) suggest that MVEs do not contain the ASGP receptor and recent immunoadsorption experiments confirm this (Mueller, S., and A. Hubbard, manuscript submitted for publication).

The results of our digitonin-shift experiments indicate that the membranes of peripheral endosomes (and internal endosomes, data not shown) have a high cholesterol content, since they shift to even a greater extent than do plasma membrane vesicles with 5′-nucleotidase activity. This is in agreement with the data of McGookey et al. (46), who observed that filipin, a molecule that alters the morphology of membranes containing cholesterol, was associated with the membranes of endosomes in which low density lipoprotein–ferritin was sequestered. Also consistent is the observation that the entry of several enveloped viruses into cells, which occurs from an endosome compartment, requires that cholesterol be a component of the fusing membrane (43).

Do Endosomes Contain ASGP Receptors?

A number of workers have reported that hepatocytes contain an intracellular pool of ASGP receptors, which is 2–20 times larger than the number of cell surface receptors (e.g., references 2 and 47–51). The conclusions are based on an increase in the observed binding activity after detergent solubilization (2), permeabilization (50), or sonication (47); on the differential effects of neuraminidase on the two receptor pools (49), and on the subcellular distribution of binding activity (48) or immuno-EM localization of receptor molecules (51). Our data demonstrate a large intracellular pool of active ASGP receptors, whose distribution on sucrose gradients does not coincide with that of a plasma membrane marker, 5′-nucleotidase, and whose relative contribution far exceeds that of the accessible ASGP binding activity, which does follow 5′-nucleotidase. Thus, the internal pool of ASGP receptors that we detect in these studies is identified by its latency and low density, and appears to be in a membrane compartment whose characteristics are strikingly similar to those of the peripheral and tubular category of internal endosomes. Both the density distribution on sucrose gradients, and parallel behavior upon exposure to low concentrations of digitonin indicate a similarity in the nature of the membrane vesicles that contain ligand and those that contain the majority of hepatocyte binding activity, particularly with regard to the cholesterol content of their membranes. ASGP receptor distribution was similar whether ligand binding or immunochemical procedures were used for their detection, which suggests that if a population of inactive receptors exists (see reference 52) it is present within the same compartment as the internal pool of active receptors. However, the results presented here do not directly prove that ligand and receptor (active or inactive) are physically in the same vesicle. Others have used different approaches to demonstrate that ASGP receptor and its internalized ligand share common endocytic compartments (e.g. references 51, 53, 54), whose overlap with those we have described will require further study. Nonetheless, the organelles that we define as endosomes by ligand introduction may be part of a stable intracellular membrane compartment into which newly internalized ligand-receptor complexes arrive and from which unoccupied receptors recycle.

We would like to thank Mr. H. Stukenbrok and Ms. S. Cameron for their assistance with the electron microscopy, Mr. T. Urquhart and Mr. T. Connolly for their photographic work, and Mrs. A. Daniel for her assistance in preparation of the manuscript.

This work was supported by National Institutes of Health grant GM29133 to A. L. Hubbard.

Received for publication 24 June 1985, and in revised form 19 August 1985.

REFERENCES

1. Wall, D. A., G. Wilson, and A. L. Hubbard. 1980. The galactose-specific recognition system of mammalian liver: the route of ligand internalization in rat hepatocytes. *Cell.* 21:79–93.
2. Steer, C. J., and G. Ashwell. 1980. Studies on a mammalian hepatic binding protein specific for asialoglycoproteins. *J. Biol. Chem.* 255:3008–3013.
3. Weigel, P. H. 1981. Evidence that the hepatic asialoglycoprotein receptor is internalized during endocytosis and that receptor recycling can be uncoupled from endocytosis at low temperature. *Biochem. Biophys. Res. Commun.* 101:1419–1425.
4. Warren, R., and D. Doyle. 1981. Turnover of the surface proteins and the receptor for serum asialoglycoproteins in primary cultures of rat hepatocytes. *J. Biol. Chem.* 256:1346–1355.
5. Dunn, W. A., D. A. Wall, and A. L. Hubbard. 1982. Use of the isolated, perfused liver in studies of receptor-mediated endocytosis. *Methods Enzymol.* 98:225–241.
6. Beaufay, H., A. Amar-Costesec, D. Thines-Sempoux, M. Wibo, M. Robbi, and J. Berthet. 1974. Analytical study of microsomes and isolated subcellular membranes from rat liver. III. Subfractionation of the microsomal fraction by isopycnic and differential centrifugation in density gradients. *J. Cell Biol.* 61:213–231.
7. Amar-Costesec, A., H. Beaufay, M. Wibo, D. Thines-Sempoux, E. Feytmans, M. Robbi, and J. Berthet. 1974. Analytical study of microsomes and isolated subcellular membranes from rat liver. II. Preparation and composition of the microsomal fraction. *J. Cell Biol.* 61:201–212.
8. Wall, D. A., and A. L. Hubbard. 1981. A pre-lysosomal membrane compartment involved in the endocytosis of asialoglycoproteins (ASGPs) by rat hepatocytes. *J. Cell Biol.* 91 (No. 5, Pt. 2):415a. (Abstr.)
9. Hubbard, A. L., D. A. Wall, and A. Ma. 1983. Isolation of rat hepatocyte plasma membranes. I. Presence of the three major domains. *J. Cell Biol.* 96:217–229.
10. Greenwood, F. C., W. H. Hunter, and J. S. Glover. 1963. The preparation of ^{131}I-labelled human growth hormone of high specific radioactivity. *Biochem. J.* 89:114–123.
11. Wall, D. A., and A. L. Hubbard. 1981. Galactose-specific recognition system of mammalian liver: receptor distribution on the hepatocyte cell surface. *J. Cell Biol.* 90:687–696.
12. Dunn, W. A., and A. L. Hubbard. 1984. Receptor-mediated endocytosis of epidermal growth factor by hepatocytes in the perfused rat liver: ligand and receptor dynamics. *J. Cell Biol.* 98:2148–2159.
13. Amar-Costesec, A., M. Wibo, D. Thines-Sempoux, H. Beaufay, and J. Berthet. 1974. Analytical study of microsomes and isolated subcellular membranes from rat liver. IV. Biochemical, physical, and morphological modifications of microsomal components induced by digitonin, EDTA, and pyrophosphate. *J. Cell Biol.* 62:717–745.
14. Hudgin, R. L., W. E. Pricer, Jr., G. Ashwell, R. J. Stockert, and A. G. Morell. 1974. The isolation and properties of a rabbit liver binding protein specific for asialoglycoproteins. *J. Biol. Chem.* 249:5536–5543.
15. Maizel, J. V. 1971. Polyacrylamide gel electrophoresis of viral proteins. *Methods Virol.* 5:179–246.
16. Bartles, J. R., L. T. Braiterman, and A. L. Hubbard. 1985. Biochemical characterization of domain-specific glycoproteins of the rat hepatocyte plasma membrane. *J. Biol. Chem.* In press.
17. Hubbard, A. L., and A. Ma. 1983. Isolation of rat hepatocyte plasma membranes. II. Identification of membrane-associated cytoskeletal proteins. *J. Cell Biol.* 96:230–239.
18. Towbin, H., T. Staehelin, and J. Gordon. 1979. Electrophoretic transfer of proteins from polyacrylamide gels to nitrocellulose sheets: procedure and some applications. *Proc. Natl. Acad. Sci. USA.* 76:4350–4354.
19. Roman, L. M., and A. L. Hubbard. 1984. A domain-specific marker for the hepatocyte plasma membrane. III. Isolation of bile canalicular membrane by immunoadsorption. *J. Cell Biol.* 98:1497–1504.
20. Hubbard, A. L., J. R. Bartles, and L. T. Braiterman. 1985. Identification of rat hepatocyte plasma membrane proteins using monoclonal antibodies. *J. Cell Biol.* 100:1115–1125.

21. Bartles, J. R., L. T. Braiterman, and A. L. Hubbard. 1985. Endogenous and exogenous domain markers of the rat hepatocyte plasma membrane. *J. Cell Biol.* 100:1126–1138.
22. Bradford, M. M. 1976. A rapid and sensitive method for the quantitation of microgram quantities of protein utilizing the principle of protein-dye binding. *Anal. Biochem.* 72:248–254.
23. Widnell, C. C., and J. C. Unkeless. 1968. Partial purification of a lipoprotein with 5′-nucleotidase activity from membranes of rat liver cells. *Proc. Natl. Acad. Sci. USA.* 61:1050–1057.
24. Hubbard, A. L., and Z. A. Cohn. 1975. Externally disposed plasma membrane proteins II. Metabolic fate of iodinated polypeptides of mouse L cells. *J. Cell Biol.* 64:461–479.
25. Rash, J. E., T. J. A. Johnson, C. S. Hudson, F. D. Giddings, W. F. Graham, and M. E. Eldefrawi. 1982. Labelled-replica techniques: post-shadow labelling of intramembrane particles in freeze-fracture replicas. *J. Microsc. (Oxf.).* 128:121–138.
26. Slot, J. W., and H. J. Geuze. 1981. Sizing of protein A-colloidal gold probes for immunoelectron microscopy. *J. Cell Biol.* 90:533–565.
27. Benacerraf, B., G. Biozzi, B. N. Halpern, C. Stiffel, and D. Mouton. 1957. Phagocytosis of heat denatured human serum albumin labelled with ^{131}I and its use as a means of investigating liver blood flow. *Br. J. Exp. Pathol.* 38:35–48.
28. Bergeron, J. J. M., J. Cruz, M. N. Khan, and B. I. Posner. 1985. Uptake of insulin and other ligands into receptor-rich endocytic components of target cells: the endosomal apparatus. *Annu. Rev. Physiol.* 47:383–403.
29. Quintart, J., P. J. Courtoy, and P. Baudhuin. 1984. Receptor-mediated endocytosis in rat liver: purification and enzymic characterization of low density organelles involved in uptake of galactose-exposing proteins. *J. Cell Biol.* 98:877–884.
30. Chao, Y. S., A. L. Jones, G. T. Hradek, E. E. T. Windler, and R. J. Havel. 1981. Autoradiographic localization of the sites of uptake, cellular transport, and catabolism of low density lipoproteins in the liver of normal and estrogen-treated rats. *Proc. Natl. Acad. Sci. USA.* 78:597–601.
31. Holtzman, E. 1976. Lysosomes: a survey. *Cell Biol. Monogr.* 3:79.
32. Khan, M. N., B. I. Posner, R. J. Khan, and J. J. M. Bergeron. 1982. Internalization of insulin into rat liver Golgi elements. Evidence for vesicle heterogeneity and the path of intracellular processing. *J. Biol. Chem.* 257:5969–5976.
33. Matlin, K. S., H. Reggio, A. Helenius, and K. Simons. 1981. Infectious entry pathway of influenza virus in a canine cell line. *J. Cell Biol.* 91:601–613.
34. McKanna, J. A., H. T. Haigler, and S. Cohen. 1979. Hormone receptor topology and dynamics: morphological analysis using ferritin-labeled epidermal growth factor. *Proc. Natl. Acad. Sci. USA.* 76:5689–5693.
35. Rodewald, R. 1973. Intestinal transport of antibodies in the newborn rat. *J. Cell Biol.* 58:189–211.
36. Hornick, C. A., R. L. Hamilton, E. Spaziani, G. H. Enders, and R. J. Havel. 1985. Isolation and characterization of multivesicular bodies from rat hepatocytes: an organelle distinct from secretory vesicles of the Golgi apparatus. *J. Cell Biol.* 100:1558–1569.
37. Ehrenreich, J. H., J. J. M. Bergeron, P. Siekevitz, and G. E. Palade. 1973. Golgi fractions prepared from rat liver homogenates. I. Isolation procedure and morphological characterization. *J. Cell Biol.* 59:45–72.
38. LaBadie, J. H., R. P. Chapman, and N. N. Aronson, Jr. 1975. Glycoprotein catabolism in rat liver. Lysosomal digestion of iodinated asialo-fetuin. *Biochem. J.* 152:271–279.
39. Pertoft, H., B. Warmegard, and M. Hook. 1978. Heterogeneity of lysosomes originating from rat liver parenchymal cells. *Biochem. J.* 174:309–317.
40. Debanne, M. T., and E. Regoeczi. 1981. Subcellular distribution of human asialotransferrin type 3 in the rat liver. *J. Biol. Chem.* 256:11266–11272.
41. Merion, M., and W. S. Sly. 1983. The role of intermediate vesicles in the adsorptive endocytosis and transport of ligand to lysosomes by human fibroblasts. *J. Cell Biol.* 96:644–650.
42. Klausner, R. D., G. Ashwell, J. van Renswoude, J. Harford, and K. Bridges. 1983. Binding of apotransferrin to K562 cells: explanation of the transferrin cycle. *Proc. Natl. Acad. Sci. USA.* 80:2263–2266.
43. Marsh, M., E. Bolzau, and A. Helenius. 1983. Penetration of Semliki Forest Virus from acidic pre-lysosomal vacuoles. *Cell.* 32:931–940.
44. Courtoy, P. J., J. Quintart, and P. Baudhuin. 1984. Shift of equilibrium density induced by 3,3′-diaminobenzidine cytochemistry: a new procedure for the analysis and purification of peroxidase-containing organelles. *J. Cell Biol.* 98:870–876.
45. Galloway, C. J., G. E. Dean, M. Marsh, G. Rudnick, and I. Mellman. 1983. Acidification of macrophage and fibroblast endocytic vesicles *in vitro*. *Proc. Natl. Acad. Sci. USA.* 80:3334–3338.
46. McGookey, D. J., K. Fagerberg, and R. G. W. Anderson. 1983. Filipin-cholesterol complexes form in uncoated vesicle membrane derived from coated vesicles during receptor-mediated endocytosis of low density lipoprotein. *J. Cell Biol.* 96:1273–1278.
47. Baenziger, J. U., and D. Fiete. 1980. Galactose and N-acetylgalactosamine-specific endocytosis of glycopeptides by isolated rat hepatocytes. *Cell.* 22:611–620.
48. Pricer, W. E., and G. Ashwell. 1976. Subcellular distribution of a mammalian hepatic binding protein specific for asialoglycoproteins. *J. Biol. Chem.* 251:7539–7544.
49. Stockert, R. J., D. J. Howard, A. G. Morell, and I. H. Scheinberg. 1980. Functional segregation of hepatic receptors for asialoglycoproteins during endocytosis. *J. Biol. Chem.* 255:9028–9029.
50. Weigel, P. H., and J. Oka. 1983. The large intracellular pool of asialoglycoprotein receptors functions during the endocytosis of asialoglycoproteins by isolated rat hepatocytes. *J. Biol. Chem.* 258:5095–5102.
51. Geuze, H. J., J. W. Slot, G. J. A. M. Strous, H. F. Lodish, and A. L. Schwartz. 1983. Intracellular site of asialoglycoprotein receptor-ligand uncoupling: double-label immunoelectron microscopy during receptor-mediated endocytosis. *Cell.* 32:277–287.
52. Fiete, D., M. D. Brownell, and J. U. Baenziger. 1983. Evidence for transmembrane modulation of the ligand-binding site of the hepatocyte galactose/N-acetylgalactosamine-specific receptor. *J. Biol. Chem.* 258:817–823.
53. Bridges, K., J. Harford, G. Ashwell, and R. D. Klausner. 1982. Fate of receptor and ligand during endocytosis of asialoglycoproteins by isolated hepatocytes. *Proc. Natl. Acad. Sci. USA.* 79:350–354.
54. Wolkoff, A. W., R. D. Klausner, G. Ashwell, and J. Harford. 1984. Intracellular segregation of asialoglycoproteins and their receptor: a prelysosomal event subsequent to dissociation of the ligand-receptor complex. *J. Cell Biol.* 98:375–381.